Polymer Chemistry

Accepted Manuscript

ROYAL SOCIETY OF CHEMISTRY

www.rsc.org/polymers

Journal Name

RSCPublishing

ARTICLE

Synthesis of amphiphilic diblock copolymers derived from renewable dextran by nitroxide mediated polymerization: towards hierarchically structured honeycomb porous films

Cite this: DOI: 10.1039/x0xx00000x

Received 00th January 2012,
Accepted 00th January 2012

DOI: 10.1039/x0xx00000x

www.rsc.org/

Senbin Chen, Marie-Hélène Alves, Maud Save and Laurent Billon*

A dextran-based macroalkoxyamine was designed by a two steps end functionalization of the initial polysaccharide. Nitroxide mediated polymerization of styrene (S) and methyl methacrylate (MMA) afforded both dextran-*b*-P(S-*co*-MMA) and dextran-*b*-PS amphiphilic linear diblock copolymers. We subsequently investigated their ability to generate honeycomb structured films using "Breath Figure" (BF) technique, a method involving the condensation of water droplets during rapid evaporation of a polymer solution under humid conditions. The quality of pore ordering of resultant films was characterized by different microscopy techniques (optical, scanning electron (SEM) and atomic force (AFM) microscopies). While non-spherical pores were observed for dextran-*b*-P(S-*co*-MMA) copolymers, an organized pattern of spherical pores was produced with dextran-*b*-PS amphiphilic copolymers leading to ordered porous bio-hybrid films. The Flory-Huggins interaction parameter χ of the couple PS/dextran is sufficiently high to induce a nanophase separation in between the pores, leading to a hierarchically structured honeycomb film based on renewable dextran block.

Introduction

Polysaccharides are an important class of biological natural polymers, its abundant, biodegradable and inexpensive characters have recently attracted remarkable attention. However, the extension of polysaccharides scope in materials applications is limited by the lack of properties inherent to natural polymers.[1] Aiming at implanting novel chemical and physical properties on polysaccharides, numerous efforts have been paid on their chemical modification by synthetic hydrophobic moieties. In particular, great successes have been achieved by utilizing the grafting strategy from the polysaccharide backbone.[1] In contrast, linear diblock copolymer structures combining polysaccharide and synthetic segments have been far less explored in comparison to grafted structures, until now.[1-2]

Three main routes towards the design of polysaccharide-based block copolymers were systematically summarized by Schatz and Lecommandoux.[2] The first route involves the end-to-end coupling reaction between polysaccharide and synthetic blocks by effective reductive amination,[3-4] popular azide-alkyne cycloaddition (CuAAC)[5-10] or oxime condensation click chemistry.[11] The second one is based on the *in vitro* enzymatic polymerization of glucosidic units initiated from end-capped synthetic polymers.[12-14] The third route relies on polymerizing the synthetic block from the polysaccharide segment adequately functionalized at its reducing end. This straightforward pathway was already reported by utilizing ring-opening polymerization (ROP),[15] conventional radical polymerization[16-17] and controlled radical polymerizations (CRP or RDRP for reversible deactivation radical polymerization), such as atom transfer radical polymerization (ATRP),[18-22] and reversible addition fragmentation chain transfer (RAFT) techniques.[23] Among the CRP techniques, nitroxide mediated polymerization (NMP) technique is interesting for its ability to create radicals

and controlling agent by a simple thermal dissociation of an alkoxyamine in the absence of either metallic catalyst or additional initiator.[24] A few examples reported the use of NMP to synthesize grafted amphiphilic copolymers based either on chitosan[25-26] or on β-cyclodextrin,[27] but to the best of our knowledge, NMP has not been implemented yet to synthesize polysaccharide-based linear amphiphilic copolymers.

The marriage of sugar based copolymers including glycopolymers or natural polysaccharides, with versatile and innovative "Breath Figure" BF method has stimulated wide interests.[28-30] For instance, honeycomb structured films prepared from amphiphilic grafted polysaccharide copolymers have been described, mainly by hydrophobically modifying cellulose.[31-32] Polystyrene comb polymers built from cellulose backbones were used to prepare honeycomb structured films.[31] It was suggested that the regularity of the porous films was influenced by the density, the length and the chemical nature of polymer grafts.[31-32] Based on regioselectively modified 2,6-(dimethylthexylsilyl) cellulose with ethylene glycol side chains, regular honeycomb structured films were also prepared by Kadla *et al.*.[33] The authors further investigated the site-specific modification of robust open framework cellulosic structures using "click" chemistry.[34] Meanwhile, by synthesizing polystyrene-*b*-poly(2-(*β*-D-galactosyloxy)ethyl methacrylate-*co*-styrene) linear amphiphilic block copolymers by NMP, our group successfully prepared lectin recognizable glyco-based biomaterials in the form of porous films relying on BF technique.[35] In the same vein, aiming at investigating the influence of the amphiphilic glyco-copolymer microstructure on the honeycomb film formation by BF method, block, statistical, and gradient copolymers carrying glycopolymers were investigated, considering that a high hydrophobic fraction is required for honeycomb film formation.[36] Mixing poly(methyl methacrylate) and amphiphilic glycopolymers was described as an approach to control the topography and the functionality of polymeric surfaces in porous films obtained by BF technique.[37]

As summarized above, honeycomb films based on natural polysaccharides mainly involved grafted copolymers. However, the microphase separation observed in amphiphilic block copolymers based on a natural hydrophilic oligosaccharide and a hydrophobic synthetic polymer was attractive to design nanostructured continuous polymer films.[5, 7] Moreover, we previously demonstrated that hierarchically structured honeycomb films can be successfully prepared through the "Breath Figure" BF process involving coil-coil diblock copolymers able to self-assemble into nano-segregated structures.[38-40]

Herein, we present for the first time a straightforward methodology for the synthesis of two different linear amphiphilic diblock copolymers based on dextran as a first block and either poly(methyl methacrylate-*co*-styrene) statistical copolymer or polystyrene as second block. For that purpose, the dextran chain end will be derivatized to introduce a SG1-based alkoxyamine able to initiate and control the subsequent polymerization of S and MMA by nitroxide mediated polymerization (NMP). Both types of diblock copolymers, *i.e.* dextran-*b*-P(S-*co*-MMA) and dextran-*b*-PS, will subsequently be subjected to BF method to fabricate honeycomb structured films. In the present work, the effect of the nature of the hydrophobic block on pore shape and organization in the honeycomb films will be investigated. The ability of a dextran-based diblock copolymer to create internal nanostructure will be discussed.

Experimental Part

Materials.

Hexylenediamine (aldrich, 98 %), $NaBH_3CN$ (aldrich, 95 %), N-hydroxysuccinimide (NHS, aldrich, 98 %), N,N′-dicyclohexylcarbodiimide (DCC, aldrich, 99 %), 1,1,1,3,3,3-hexamethyldisilazane (HMDS, Aldrich, 99.9 %), triethylamine (TEA, aldrich, 99 %), 1,3,5-trioxane (aldrich, 99 %) and trifluoroacetic acid (TFA, aldrich, 99 %) were used as received. N-(2-Methylpropyl)-N-(1- diethylphosphono- 2,2-dimethylpropyl)-O-(2-carboxylprop-2-yl) hydroxylamine initiator (so-called BlocBuilder®, 99 %, named BB) and the N-tert-butyl-N-(1-diethyl phosphono-2,2-dimethylpropyl) nitroxide (SG1, 88.4 %) were kindly provided by Arkema (France). Dextran (Dextran 4 Techn. Grade, Mn = 2600 $g.mol^{-1}$, M_w/M_n = 1.46, and number-average degree of polymerization DPn = 16 was determined by SEC using H_2O as eluent in previous report) was purchased from Serva Electrophoresis. Diethyl phosphite (aldrich, 98 %) was distilled before use, styrene (S, aldrich, 99 %) and methyl methacrylate (MMA, aldrich, 98.5 %) were freshly deinhibited using an inhibitor remover. Unless otherwise indicated the other chemicals were used without further purification.

Characterization Methods.

NMR spectra were recorded using a Bruker 400 MHz spectrometer at 25 °C. ^1H and ^{31}P measurements were performed at frequencies of 400.13 and 161.98 MHz, respectively. $CDCl_3$, DMSO-d_6 or a mixture of DMSO-d_6 with $CDCl_3$ or pyridine-d_5 was used as solvent.

The polymers were characterized of by Size Exclusion Chromatography (SEC) running in THF at 30 °C (flow rate: 1 $mL.min^{-1}$) or in DMF + LiCl (5 $g.L^{-1}$) at 50 °C (flow rate: 0.5 $mL.min^{-1}$) as eluent, equipped with a Viscotek VE 1121 automatic injector, three columns (Waters HR0.5, HR2 and HR0.5), and a differential refractive index detector (Viscotek VE3580). SEC columns were calibrated against PMMA and PS standards for dextran-*b*-P(S-*co*-MMA) and silylated dextran-*b*-PS, respectively.

Pictures from optical microscopy were taken in reflection with a Leica DM/LM microscope equipped with ×100 optic and a Leica DFC280 video camera. The regular image treatments were performed with the Image Manager IM50 software. The 2-Dimensional Fast Fourier Transform was performed with the 2D FFT function available on Igor Pro® software.

Scanning electron microscopy (SEM) images were achieved using an Electroscan E3 scanning microscope, operated at an

accelerating voltage of 25 keV. Electron micrographs of the sample were recorded at different magnifications, ranging from 500 to 3000.

Images by atomic force microscopy (AFM) were performed on the Multi mode 8 (BrükerNano) using triangular silicon nitrid cantilevers from Brüker-probe (ScanAsyst-Air). The images were scanned in PeakForce QNM (Quantitative NanoMechanics), an extension of Peak Force TappingTM mode, under ambient conditions. The height channel displays topographical images of the samples and the peak force below the baseline shows an adhesion map of sample.

Synthesis of End-Group Aminated Dextran: Dextran-NH_2.

Dextran-NH_2 was synthesized according to literature method with slight modification.[41] Dextran (1.0 g, M_n = 2600 g.mol^{-1}, 0.4 mmol) dissolved in 2 mL distilled water, was treated with hexylenediamine (1 mL, 8 mmol, 20 eq.) and stirred for 2 h. $NaBH_3CN$ (125 mg, 2 mmol) was then added, and the reaction mixture was continuously stirred at room temperature overnight. The solution was precipitated in MeOH two times, after filtration and dried under vacuum, the obtained product dextran-NH_2 was characterized by ^{1}H NMR spectrometry.

Synthesis of macro initiator: Dextran-SG1.

The preparation of a BlocBuilder® derived alkoxyamine bearing a N-succinimidyl (NHS) ester group (named NHS-BB in) was synthesized according to reference.[42] In a nitrogen conditioned flask equipped with a magnetic stirrer, BlocBuilder® (5 g, 13.1 mmol) and N-hydroxysuccinimide (1.81 g, 15.7 mmol) were dissolved in THF (20 mL). After cooling to 0 °C, a degassed solution of DCC (3 g, 14.4 mmol) in THF (5 mL) was added. The reaction was stirred at 0 °C for 1.5 h and then at room temperature for one night, the reaction mixture was filtered in order to remove the precipitated N,N'-dicyclohexylurea (DCU), the solution was concentrated under reduced pressure and precipitation was performed in pentane. The obtained solid was dried and used for the functionalization of dextran-NH_2 without further purification.

Freshly synthesized dextran-NH_2 (1.0 g, 0.33 mmol) and NHS-BB (0.8 g, 1.7 mmol, 5 eq.) were mixed together in 5 mL dried DMSO, then stirred at RT for 1 day. The reaction solution was subsequently precipitated in methanol. The white precipitation (dextran-SG1) was collected and dried under vacuum, then characterized by ^{1}H and ^{31}P NMR. The average functionality of dextran-SG1 given by 1H NMR (65 %, see calculation in supporting information) was chosen for further calculation of alkoxyamine concentration. The average value provided by 31P NMR is in the same range (61 %, see ESI) but was not considered due to the additional error introduced by considering the mass of the introduced sample.

Copolymerization of MMA and styrene mediated by Dextran-SG1.

Solution copolymerization was mediated by dextran-SG1 at 90 °C in DMSO. A mixture of MMA (2.5 g, 2.5 × 10^{-2} mol), styrene (0.78 g, 7.5 × 10^{-3} mol), SG1 (0.002 g, 6.5 × 10^{-6} mol), dextran-SG1 (0.30 g, functionality = 65%, 6.5 × 10^{-5} mol of alkoxyamine), 1,3,5-trioxane (127 mg, 1.4 × 10^{-3} mol) and 15 mL DMSO was typically transferred into a flask sealed with rubber septum, deoxygenated by nitrogen bubbling for 30 min at room temperature, then immersed in a thermostated oil bath. Samples were periodically withdrawn to follow the monomer consumption using 1,3,5-trioxane as an internal reference by ^{1}H NMR. The reaction was stopped by plunging the flask into liquid nitrogen. The polymer was subsequently precipitated twice into methanol in order to eliminate the residual monomer and 1,3,5-trioxane. The recovered polymer was dissolved in DMSO/DMF (1/2, v/v) and further extensively dialyzed against distilled water using a dialysis tubing (molecular weight cut-off: 6000-8000 g.mol^{-1}) for 3 days to remove free dextran. The obtained polymers were dried and characterized by ^{1}H NMR and SEC.

The molar mass and composition of purified dextran-*b*-P(S-*co*-MMA) were evaluated by ^{1}H NMR (**Figure 3**) from the ratios of the intensities of the three following peaks: 4.70 ppm (15 anomeric protons of the dextran backbone), 6.50-7.60 ppm (5*n*H aromatic protons of PS, with *n* being the degree of polymerization of PS) and 0.08-2.10 ppm (5*m*H CH_3-, -CH_2- of PMMA, 3*n*H -C*H*-, -CH_2- of PS, with *m* being the degree of polymerization of PMMA, 38H of SG1 group of dextran-SG1) (see calculation in Electronic Supplementary Information (ESI)).

Polymerization of styrene mediated by Dextran-SG1.

Solution polymerization of styrene was mediated by dextran-SG1 at 120 °C in the mixture of DMSO/DMF. Typically, the solution polymerization of styrene (3.0 g, 2.9 × 10^{-2} mol) was carried out using dextran-SG1 (0.30 g, functionality = 65 %, 6.5 × 10^{-5} mol), DMSO (7mL), DMF (13 mL) and 1,3,5-trioxane (127 mg, 1.4 × 10^{-3} mol) as an internal reference for the measurement of styrene consumption via ^{1}H NMR. A stock solution was transferred into flask sealed with rubber septum, deoxygenated by nitrogen bubbling for 30 minutes at 0 °C, then immersed in a thermostated oil bath. Samples were periodically withdrawn to follow the monomer consumption by ^{1}H NMR. The reaction was stopped by plunging the flask into liquid nitrogen. The polymer was subsequently precipitated twice into ethanol in order to eliminate the residual monomer and 1,3,5-trioxane. The obtained precipitation was dissolved in DMSO/DMF (1/2, v/v) and further extensively dialyzed against distilled water using a dialysis tubing (molecular weight cut-off: 6000-8000 g.mol^{-1}) for 3 days to remove free dextran. The obtained polymers were dried and characterized by ^{1}H NMR and SEC.

The molar mass of pure dextran-*b*-PS was evaluated by ^{1}H NMR (**Figure 5**B) from the ratios of the intensities of the two following peaks: at 5.21 ppm (15 anomeric protons of the dextran backbone), 0.90-2.45 ppm (3*n*H -C*H*-, -CH_2- of PS,

with *n* being the degree of polymerization of PS and 38H of SG1 group of dextran-SG1).

SILYLATION OF DEXTRAN AND DEXTRAN-*b*-PS.

Silylation reaction of OH groups in the dextran backbone was performed according to literature method [43] using 1,1,1,3,3,3-hexamethyldisilazane as protecting agent. Typically, dried dextran-*b*-PS was dissolved by freshly dried DMSO/THF (1/1, v/v) in a N_2-purged flask, equipped with a stopcock and connected to an oil valve for ammoniac evolution, then HMDS (4 eq to OH groups of dextran) and TEA (0.2 eq to OH groups of dextran) were added. The reaction medium was subsequently stirred at 60 °C for 48h. Then the reaction solution was concentrated and recovered by precipitation in EtOH to afford expected silylated-dextran-*b*-PS. The degree of silylation for different block polymers was ranging between 85 and 100 % (see example in **Figure S2** in ESI).

Preparation of copolymer porous films.

The preparation of the porous structure using the "Breath Figure" BF approach was conducted in a Perspex glove box with relative humidity (RH) control, between 50 and 75% of RH at 20 °C. The humid air flow was set at 2 $L.min^{-1}$. 5-15 mg of polymers were first stirred overnight in 1mL of $CHCl_3$. The resultant cloudy solution was then sonicated for 15 min to form a homogeneous solution before casting onto a glass substrate in the Perspex box. The porous films were usually obtained within 30 seconds due to the high solvent volatility.

Results and discussion

The biohybrid block copolymers containing a renewable polysaccharide block and a synthetic polymer block were designed by a three steps procedure. First, the initial dextran was end-modified in two steps to introduce the SG1-based alkoxyamine (**Scheme 1**) before the further chain extension of the dextran-SG1 macronitiator by NMP polymerization of styrene and methyl methacrylate.

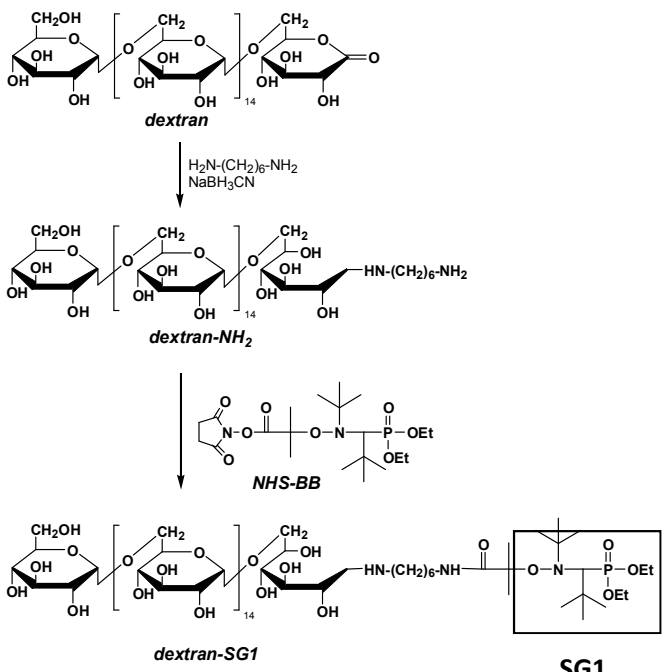

Scheme 1. Route for synthesis of dextran-SG1 macroalkoxyamine.

SYNTHESIS OF DEXTRAN-SG1 MACRO-ALKOXYAMINE.

The synthesis of dextran-SG1 was realized as described in **Scheme 1**, without employing any protection/deprotection strategy or metal catalyst.

The *ω*-functionalization of dextran was primarily tailored by introducing an amine group *via* effective reductive amination. After purification of the amino-dextran (dextran-NH_2) by precipitating the polymer into methanol, the recovered white solid was analysed by proton NMR (**Figure 1**). The effective incorporation of hexylenediamine was first evidenced by the appearance of the peaks at chemical shifts of 1.35 ppm (–NH-CH_2-$\underline{CH_2}$-CH_2-CH_2-$\underline{CH_2}$-CH_2-NH_2) and 1.22 ppm (–NH-CH_2-CH_2-$\underline{CH_2}$-$\underline{CH_2}$-CH_2-CH_2-NH_2) characteristic of eight protons of hexylenediamine moiety (**Figure 1C**). The protons of –NH-$\underline{CH_2}$ and -$\underline{CH_2}$-NH_2 methyne groups are embedded in the signals of DMSO and dextran. In agreement with previous results,[21, 23, 41] the reductive amination of dextran with a molar excess of hexylenediamine in the presence of sodium cyanoborohydride was quantitative. The presence of an amine group in *ω*-position of dextran chain was further exploited to generate the dextran-SG1 macroalkoxyamine by amidation reaction between an activated ester (NHS-BB) and an amine group. For that purpose, the BlocBuilder® derived alkoxyamine bearing a N-succinimidyl (NHS) ester group (named BB-NHS in **Scheme 1**) was first synthesized according to reference.[42]

After the purification step by precipitation into methanol, the

Journal Name RSCPublishing

ARTICLE

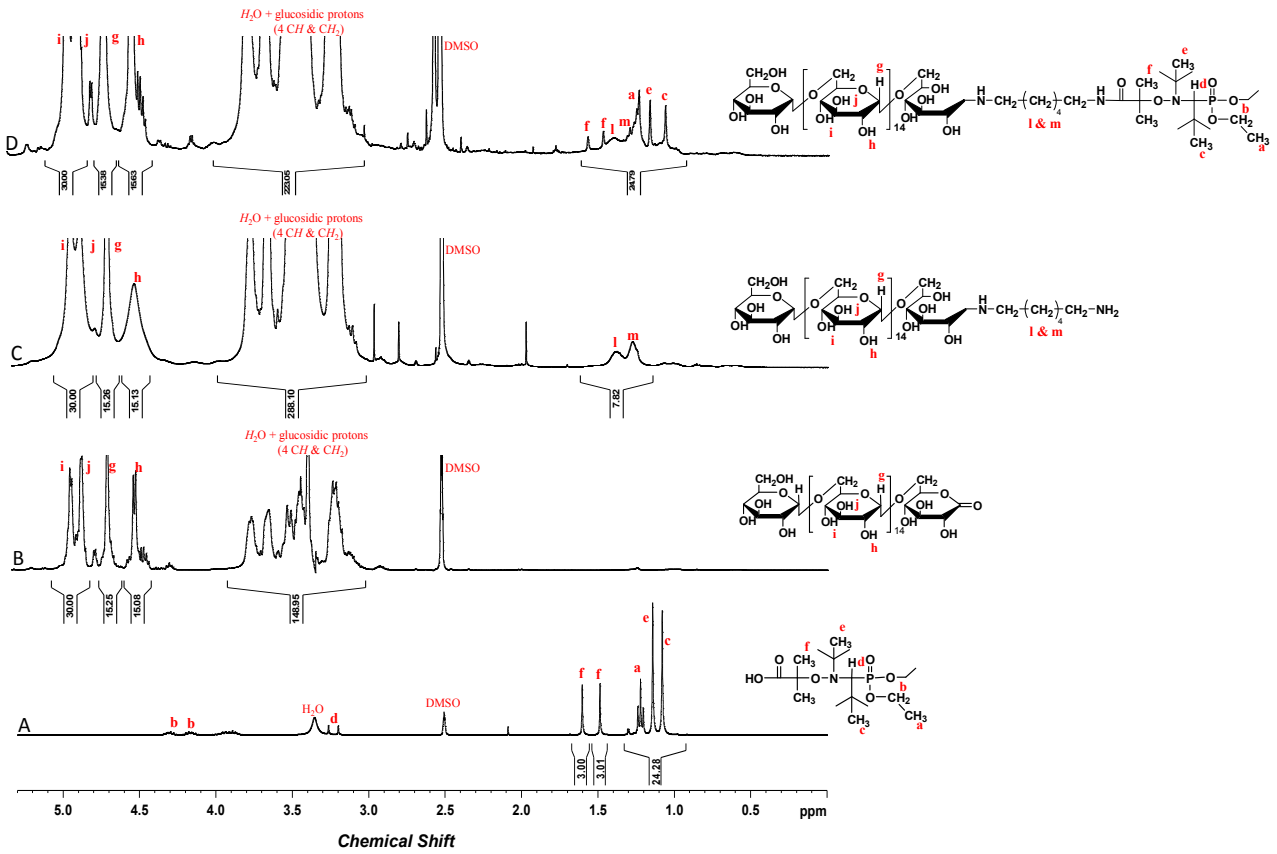

Figure 1. Overlay of ^{1}H NMR spectra recorded in DMSO-d_6 at 25°C of: A: BlocBuilder®, B: initial dextran, C: dextran-NH_2, D: dextran-SG1.

obtained white solid (dextran-SG1) was analysed by ^{1}H NMR (**Figure 1D**). The evidence of successful incorporation of SG1-based alkoxyamine was provided by the appearance of the typical peaks of BlocBuilder® at chemical shifts ranging between 1.0 and 1.62 ppm (**Figure 1A** & **D**). The degree of functionalization was subsequently determined from relative integration of dextran-SG1 end group peaks (from 0.91 to 1.62 ppm) and the peak of anomeric protons of dextran (from 4.58 to 4.76 ppm) (**Figure 1D**). The degree of functionalization was calculated as being 65 % (detail of calculation in ESI). Thanks to the phosphorous atom of the *N*-*tert*-butyl-*N*-(1-diethyl phosphono-2,2-dimethylpropyl) nitroxide, so-called SG1, it was also possible to calculate the degree of functionalization of dextran-SG1 by ^{31}P NMR analysis. A degree of functionalization of 61 % was calculated from the integrations of both peaks at chemical shift of δ = 27.0 ppm and δ = 8.4 ppm corresponding respectively to dextran-SG1 and the freshly distilled diethyl phosphite as internal reference (**Figure S1** in ESI). These both results are in good agreement and reveal the successful chemical modification of dextran by the SG1-based alkoxyamine.

Copolymerization of S/MMA mediated by Dextran-SG1. Although successful syntheses of linear block copolymers containing dextran have been previously reported by different controlled radical polymerization (CRP) techniques, the employed strategies required either protection/deprotection steps of dextran prior to ATRP polymerization carried out in homogeneous media,[21] or relied on RAFT polymerization performed in aqueous dispersed media (emulsion polymerization), which resulted in higher dispersity values.[23] A combination of oxime click reaction and ATRP has been recently applied to synthesize dextran-*b*-poly(2-(dimethylamino)ethyl methacrylate) diblock copolymer in homogeneous media (DMSO solvent) but in the absence of polysaccharide protection/deprotection steps.[22] The purpose of the present work is first to synthesize dextran-*b*-(PMMA-*co*-S) block copolymers by NMP in DMSO as both dextran and PMMA blocks are soluble in this solvent. The absence of

metallic catalyst in NMP is advantageous to reduce the purification steps of the final copolymer. According to literature, the addition of a minimum of 4-10 mol-% of styrene is required for controlling MMA polymerization initiated by BlocBuilder® alkoxyamine,[44-45] by reducing the fraction of irreversible terminations between the propagating radicals and β-hydrogen transfer from a propagating radical to a free-SG1 nitroxide.[44, 46] In the present work, the initial fraction of styrene (f_S) was set at 23 mol-% for the synthesis of dextran-*b*-(PMMA-*co*-S) block copolymers by NMP carried out in DMSO at 90 °C (**Table 1**). The initial experimental conditions, final monomer conversions and features of the synthesized copolymers are gathered in **Table 1**.

Figure 2 shows linearity of first order kinetic plot for the S/MMA copolymerization initiated by dextran-SG1 macroalkoxyamine, which is indicative of a constant concentration of propagating radicals. Through linear trend of the number-average molar mass (M_n) of the copolymer versus conversion, the controlled nature of polymerization was further indicated by the shift of the unimodal SEC traces towards lower elution volume together with the decrease of the copolymer dispersity values ($Đ = M_w/M_n$) as conversion increases (**Figure 2**). It can be noticed that reasonable average dispersity values

Table 1. Experimental conditions and results for synthesis of dextran-*b*-P(S-*co*-MMA) and dextran-*b*-PS block copolymers by NMP.

Expt	$[I]_0$ [c] *mmol.L^{-1}*	$[MMA]_0$ *mol.L^{-1}*	$[S]_0$ *mol.L^{-1}*	f_S [d]	*Conv* [e]	F_S [f]	$M_{n,theo}$ [g] *g.mol^{-1}*	$M_{n,NMR}$ [h] *g.mol^{-1}*	$M_{n,SEC}$ [i] *g.mol^{-1}*	$Đ$	$\frac{M_{n,theo}}{M_{n,SEC}}$	*Final copolymer*
1[a]	3.5	1.35	0.4	0.23	8.4	0.29	6 700	12 000	11 100[j]	1.61	0.56	Dext-*b*-P(S_{26}-*co*-MMA_{59})
2[a]	3.5	1.35	0.4	0.23	19.5	0.28	12 400	17 300	16 900[j]	1.59	0.71	Dext-*b*-P(S_{47}-*co*-MMA_{111})
3[a]	3.5	1.35	0.4	0.23	29.5	0.26	17 400	25 200	20 500[j]	1.54	0.69	Dext-*b*-P(S_{67}-*co*-MMA_{181})
4[a]	3.5	1.35	0.4	0.23	40.1	0.24	22 600	28 400	28 400[j]	1.55	0.80	Dext-*b*-P(S_{71}-*co*-MMA_{211})
5[b]	2.8	0	1.24	1.00	17.1	1	10 400	15 300	18 600[k]	1.56	0.68	Dext-*b*-PS_{123}
6[b]	2.8	0	1.24	1.00	24.9	1	14 100	19 900	21 700[k]	1.55	0.71	Dext-*b*-PS_{167}
7[b]	2.8	0	1.24	1.00	35.8	1	19 100	25 600	23 400[k]	1.55	0.74	Dext-*b*-PS_{220}
8[b]	2.8	0	1.24	1.00	49.4	1	25 300	29 000	31 700[k]	1.54	0.87	Dext-*b*-PS_{254}

[a] Polymerization carried out in DMSO (15 mL) at 90 °C, $[M]_0/[I]_0 = 500$, 10 mol % of free SG1 was added. [b] Polymerization carried out in DMSO (7 mL) and DMF (13 mL) at 120 °C, with $[M]_0/[I]_0 = 440$. [c] Initial concentration of alkoxyamine initiator calculated as follows: $[I]_0 = ((m_{dextran\text{-}SG1}/M_{n,dextran\text{-}SG1}) \times 0.65)/V$, as the alkoxyamine functionality of dextran-SG1 is 65 %. [d] Initial molar fraction of styrene in the co-monomer mixture. [e] Overall monomer conversion from ^{1}H NMR. [f] Molar fraction of styrene in the final copolymers calculated by ^{1}H NMR. [g] Theoretical number-average molar mass was evaluated from the following equation: $M_{n,theo} = M_{n,dextran\text{-}SG1} + conv. \times ([M]_0/[I]_0) \times M_M$. [h] M_n determined from ^{1}H NMR. [i] M_n from SEC in DMF. [j] M_n of dextran-*b*-P(MMA-*co*-S) copolymer measured by SEC in DMF. [k] M_n of dextran-*b*-PS copolymer deduced from M_n of silylated dextran-*b*-PS measured by SEC in THF.

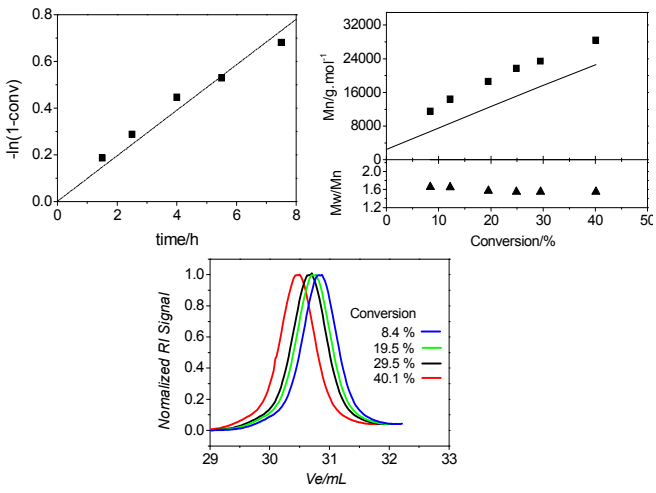

Figure 2. NMP copolymerization of MMA/S initiated by dextran-SG1 (T = 90 °C, DMSO), (top left) first-order kinetic plots, (top right) $M_{n,SEC}$ (squares), dispersity $Đ$ (triangles) and $M_{n,theo}$ (straight line) versus conversion, (bottom) evolution of the SEC traces (Expts 1-4 of **Table 1**).

were obtained ($Đ$ = 1.54 – 1.61 in **Table 1**) if bearing in mind that initiation took place from a polydisperse dextran-SG1 macroalkoxyamine ($Đ_{dextran}$ = 1.46).

As reported in **Table 1**, the values of the experimental molar masses are systematically above the theoretical ones ($M_{n,theo}/M_{n,SEC} < 1$) despite the fact that the functionality of the dextran-SG1 macro-alkoxyamine was considered in the calculation of theoretical molar masses. This reveals incomplete consumption of dextran-SG1 alkoxyamine but the initiation efficiency increases with monomer conversion (see increasing values of $M_{n,theo}/M_{n,SEC}$ in **Table 1**). The values of the styrene fraction in the final dextran-*b*-P(S_n-*co*-MMA_m) copolymers (F_S) were calculated on the basis of the degrees of polymerization of each monomer, the later *n* and *m* values being calculated from the integrations of proton NMR peaks of the purified copolymers (see **Figure 3** and calculation in ESI). The experimental values of F_S (**Table 1**) are in accordance with the theoretical F_S values calculated from Lewis-Mayo equation versus conversion (see **Figure S3** in ESI for theoretical plots using $r_S = 0.489$, $r_{MMA} = 0.493$).[47]

Polymerization of styrene mediated by Dextran-SG1. In this part, the ability of dextran-SG1 macro-alkoxyamine was investigated to efficiently initiate and control styrene polymerization to afford dextran-*b*-PS linear block copolymers. A previous investigation of dextran-*b*-PS copolymer self-assembly as a function of both PS weight fraction and nature of

solvent highlighted the incomplete solubility of such diblock copolymers in DMSO, THF and water.[19] In the present work, the dextran-*b*-PS diblock copolymers were synthesized by chain extension of dextran-SG1 *via* styrene NMP carried out at 120°C in a mixture of DMF/DMSO (65/35, v/v) to fully solubilise the dextran-*b*-PS (Expts 5-8 in **Table 1**).

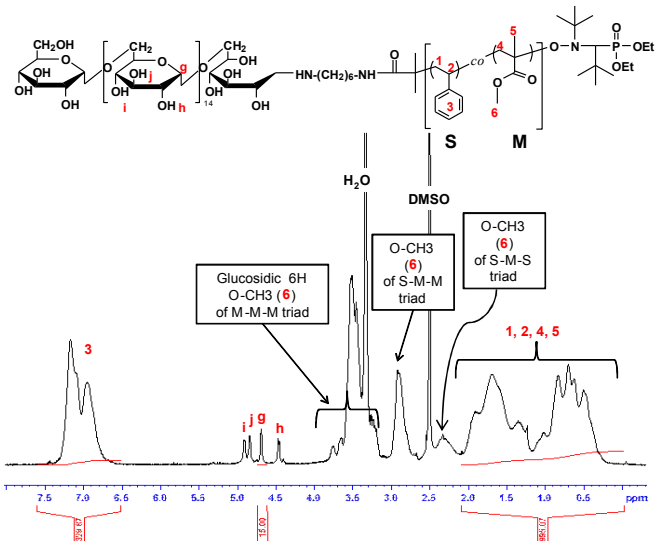

Figure 3. ^{1}H NMR spectrum of dextran-*b*-P(S-*co*-MMA) recorded at 25°C in DMSO-d_6 (Expt 3 of **Table 1**).

As evidenced in **Figure 4**, styrene polymerization mediated by dextran-SG1 highlighted a linear relationship. In a similar manner as for S/MMA NMP copolymerization described above, NMP of styrene mediated by dextran-SG1 exhibited features of a controlled polymerization. Indeed, **Figure 4** shows linear relationship of both logarithmic monomer conversion versus time and M_n versus conversion plots, with monomodal SEC chromatograms of dextran-*b*-PS copolymers (Đ ~ 1.55).

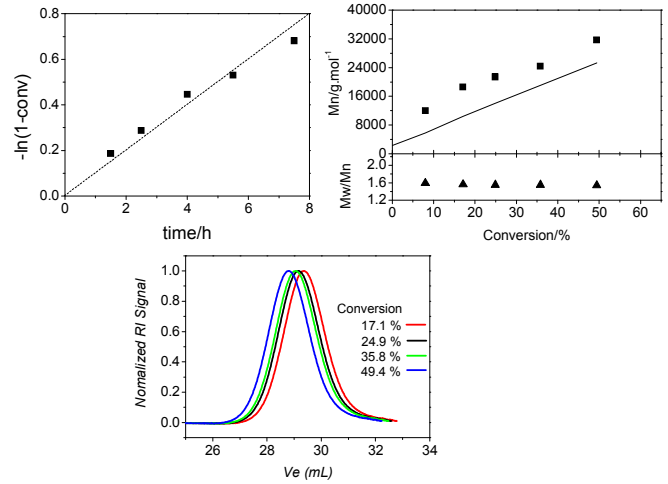

Figure 4. NMP polymerization of S initiated by dextran-SG1 (T = 120 °C, DMF/DMSO (65/35, v/v)): (top left) first-order kinetic plots, (top right) $M_{n,SEC}$ (squares), dispersity *Đ* (triangles) and $M_{n,theo}$ (straight line) versus conversion, (bottom) evolution of the SEC traces (Expts 5-8 of **Table 1**).

As observed for the synthesis of dextran-*b*-P(S-*co*-MMA) copolymers, an increase of the dextran-SG1 alkoxyamine initiation efficiency with monomer conversion is observed for NMP of styrene (see **Table 1**, the value of $M_{n,theo}/M_{n,SEC}$ increases from 0.68 to 0.87). Finally, the deviating M_n and the relatively high dispersity values could be as a consequence of the combination of both factors, *i.e.* the initial dispersity value of the dextran-SG1 ($Đ_{dextran}$ = 1.46) and the incomplete consumption of dextran-SG1 alkoxyamine after chain extension, which leads to the presence of 10 to 30% of residual dextran in block copolymers.

It is worth noting that the ^{1}H NMR peaks of dextran were extremely broadened and not easily observed for the dextran-*b*-PS copolymer recorded in the mixture of DMSO-d_6 and $CDCl_3$ (**Figure 5A**); by analogy with previous study.[27] Signals of dextran appeared along with aromatic protons in PS chain when a mixture of DMSO-d_6 and pyridine-d_5 were employed as solvent (**Figure 5B**). Aiming at further clearly identifying each signal, a drop of trifluoroacetic acid (TFA) was added in the DMSO-d_6 and pyridine-d_5 polymer solution, resulting in disappearance of peaks corresponding to OH groups in dextran backbone and water (**Figure 5C**).

PREPARATION OF HONEYCOMB STRUCTURED POROUS FILMS. The synthesized dextran-*b*-P(S-*co*-MMA) and dextran-*b*-PS diblock copolymers were used to elaborate honeycomb structured films using BF approach. Optical microscopy, scanning electron microscopy (SEM) and atomic force microscopy (AFM) were the techniques of choice to examine the pore organization at the surface of the polymeric films.

Previous studies indicated that the regularity of pores fabricated by amphiphilic copolymers were dependent on the ratio of the volumic fractions of both hydrophobic and hydrophilic moieties. This is due to the disturbing water condensation effect inside the hydrophilic part of inverse polymeric micelles formed in the organic solvent required for BF method.[28, 30, 48-49] As described in the first part of this work, a series of amphiphilic block copolymers with different length of hydrophobic block were synthesized. **Figure 6** presents images of porous films prepared at constant relative humidity of 60 % from chloroform solutions of different copolymers with an increasing length of the hydrophobic P(S-*co*-PMMA) block.

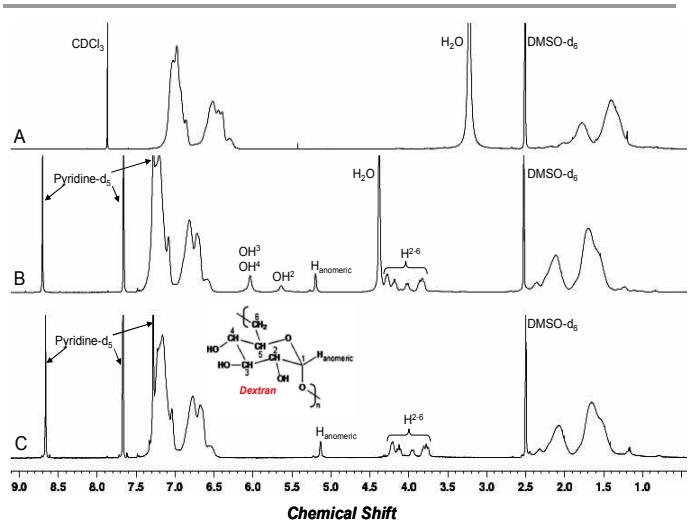

Figure 5. Overlay view of ^{1}H NMR spectra of dextran-*b*-PS recorded at 25°C in different solvents: (A) DMSO-d_6/$CDCl_3$ (2/1, v/v), (B) DMSO-d_6/pyridine-d_5 (3/7, v/v), (C) DMSO-d_6/pyridine-d_5 (3/7, v/v) + a drop of TFA.

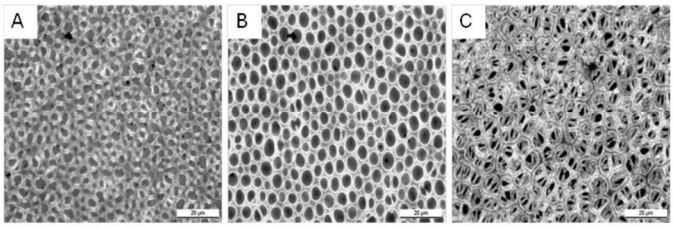

Figure 6. Optical microscopy pictures of porous films obtained from (A) Dext-*b*-P(S_{47}-*co*-MMA_{111}), (B) Dext-*b*-P(S_{67}-*co*-MMA_{181}) and (C) Dext-*b*-P(S_{71}-*co*-MMA_{211}) in $CHCl_3$ (5 g.L^{-1}) at relative humidity of 60% (scale bare = 20 µm).

Under such experimental conditions, no ordered pattern of pores can be generated in all the films of dextran-*b*-P(S-*co*-PMMA) copolymer and non-spherical pores are observed.

It is well known that BF process is highly sensitive towards relative humidity.[28-29, 50] Therefore, the relative humidity levels were ranged between 50 and 75 % while keeping all other parameters constant, as depicted in **Figure 7**. As expected, the pore size increased with increasing relative humidity favouring water condensation onto the cold film surface. Nevertheless, the pores are not organized in a structured pattern.

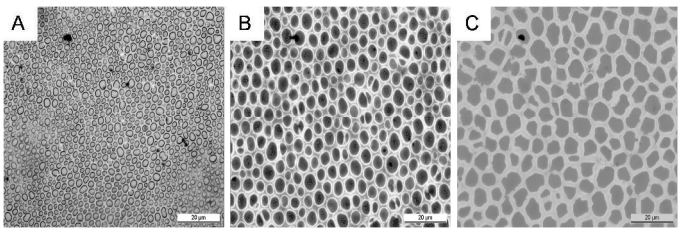

Figure 7. Optical microscopy pictures of porous films prepared from Dext-*b*-P(S_{67}-*co*-MMA_{181}) in $CHCl_3$ at 5 g.L^{-1} at varying relative humidity: (A) 50 %, (B) 60 % and (C) 75 % (scale bare = 20 µm).

During BF process, it has been well-established that the pore size is also influenced by the polymer concentration of amphiphilic copolymer.[48, 51] Dextran-*b*-P(S-*co*-MMA) copolymer solutions of different concentrations ranging between 5 and 15 g.L^{-1} were casted under relative humidity of 60 % (**Figure 8**). The obvious decrease of pore diameter from *ca*. 5 µm down to 2 µm was observed when increasing copolymer concentration from 5 to 15 g.L^{-1}.

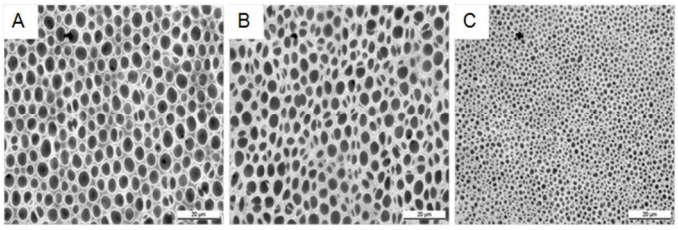

Figure 8. Optical microscopy pictures of porous films from obtained from Dext-*b*-P(S_{67}-*co*-MMA_{181}) in $CHCl_3$ (5 g.L^{-1}) at relative humidity of 60 % and varying concentration, (A): 5 g.L^{-1}, (B): 10 g.L^{-1} and (C): 15 g.L^{-1} (scale bare = 20 µm).

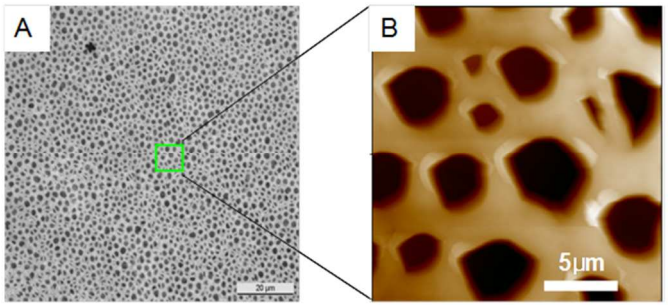

Figure 9. Optical microscopy (A) (scale bare = 20 µm) and AFM (B) pictures of porous films obtained from Dext-*b*-P(S_{71}-*co*-MMA_{211}) (Expt 4 in **Table 1**) in $CHCl_3$ (15 g.L^{-1}) at relative humidity of 70 %.

The non-spherical shape of the pores was confirmed by AFM imaging of the dextran-*b*-P(S_{71}-*co*-MMA_{211}) porous films (**Figure 9**).

In the BF process involving condensation of water droplets at the surface of polymer solution, the pore morphology can be influenced by surface tensions of water droplet (γ_w), polymer solution (γ_p) and interfacial tension between the polymer solution and water droplets ($\gamma_{w/p}$).[52-53] From the spreading coefficient expressed by Harkins *et al.*[54] ($S = \gamma_p - (\gamma_w + \gamma_{w/p})$, the nature of the polymer might influence the shape of the condensed water droplets *via* the value of $\gamma_{w/p}$.[53] Wang *et al.*[55] reported lower interfacial tension between PMMA and aqueous phases in comparison with interfacial tension between PS and aqueous phases. In addition the lower hydrophobicity of PMMA in comparison with PS can reduce the fast polymer precipitation required in the BF process.[29, 56] Such different behaviour might favour coalescence of water droplets during dextran-*b*-P(S-*co*-MMA) films formation. Indeed, non-spherical and larger pore sizes (D ~ 2 - 5 µm) are observed for dextran-*b*-P(S-*co*-MMA) porous films while dextran-*b*-PS amphiphilic copolymers are able to generate smaller spherical pores (D ~ 1 - 3 µm) as depicted below (**Figure 10C**, **Figure 11**, **Figure 12**).

We further examined the preparation of films cast from solutions of dextran-*b*-PS copolymer in chloroform. Indeed, polystyrene homopolymer or PS-based diblock copolymers are

popular candidates to prepare honeycomb structured films.[29, 50, 57-58] Taking advantage of amphiphilic block copolymers containing PS as hydrophobic block, honeycomb structured films have been successfully prepared by several groups.[49, 59-65] As displayed in **Figure 10**, the PS block length strongly influences the pore ordering. Indeed, an ordered pattern of pores was obtained in the case of dextran-*b*-PS_{254} exhibiting the longest PS block, with average pore of size of 2 µm (**Figure 10**C).

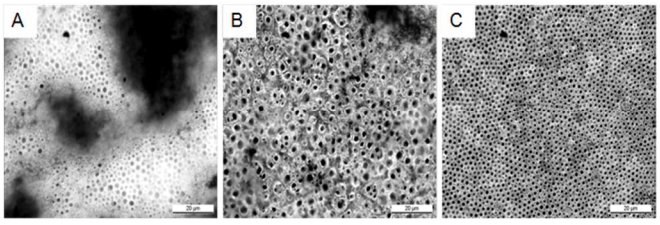

Figure 10. Optical microscopy pictures of porous films from obtained from (A) Dext-*b*-PS_{123} (Expt 5 of **Table 1**) (B) Dext-*b*-PS_{167} (Expt 6 of **Table 1**) (C) Dext-*b*-PS_{254} (Expt 8 of **Table 1**) $CHCl_3$ solutions (15 $g.L^{-1}$) at relative humidity of 60% (scale bare = 20 µm).

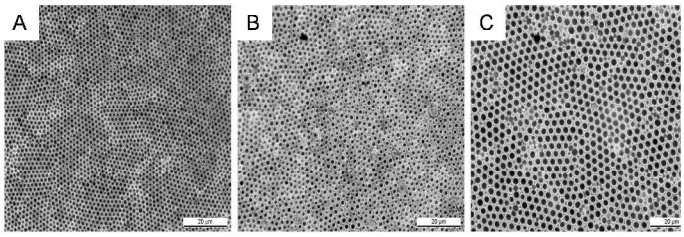

Figure 11. Optical microscopy pictures of porous films obtained from Dext-*b*-PS_{254} in $CHCl_3$ at 15 $g.L^{-1}$ and varying humidity (A): 50 %, (B): 60 % and (C): 75 % (scale bare = 20 µm).

Solutions of dextran-*b*-PS_{254} in chloroform were casted at different humidity levels ranging from 50 % to 75%. As expected, the optical microscopy images of **Figure 11** show an increase of pore diameters from $D \sim 1.3$ µm up to ~ 3.0 µm with increasing relative humidity RH from 50 % to 75 %.

The hexagonal arrangements of pores in dextran-*b*-PS_{254} honeycomb films was confirmed by optical microscopy and SEM images in **Figure 12A**. A spherical shape of pores was also observed by SEM and AFM in dextran-*b*-PS_{254} films (inset **Figure 12A** and **Figure 12B**). Here, we can mention that the ratio between hydrophobic/hydrophilic blocks has already been investigated by Malkoch *et al*. to show the importance of the level of hydrophobicity of amphiphilic copolymers in the preparation of porous films by BF process.[66] For a poly(ε-caprolactone)-*b*-poly(ethylene glycol) block copolymer (PEG_{50}-*b*-PCL_{60}) with 77 wt-% of hydrophobic component, a partial coverage of the glass substrate was observed while the more hydrophobic PEG_{50}-*b*-PCL_{240} copolymer with 93 wt-% of hydrophobic component enabled the formation of a homogeneous porous film with a diameter of circular pores of *ca.* 3 µm. The same trend is observed in the present study with dextran-*b*-PS_{123} and dextran-*b*-PS_{254}, respectively.

A nanostructuration in between the pores is observed in dextran-*b*-PS_{254} honeycomb film (**Figure 12C**), leading to a hierarchically structured honeycomb film. This suggests that the Flory-Huggins interaction parameter (χ) of the PS/dextran couple is high enough to induce spontaneously nanophase separation during the fast solvent evaporation. Borsali et *al.*[7] described the self-assembly of block copolymers composed of naturally derived oligosaccharides coupled to a silicon-containing polystyrene derivative (poly(para-trimethylsilylstyrene)). These block copolymers exhibiting high χ values, so low degrees of polymerization (DP) of both the oligosaccharides and the PTMSS blocks (DP ≈ 7 and 26, respectively) were sufficient to enable the formation of nano-domains of oligosaccharides of 5 nm size and row spacing between features of 11.4 nm, both associated to the length of the PTMSS.[7] In the present work, despite the very fast process of film formation (less than 2 minutes) and the absence of any annealing step, we observed by AFM the formation of 8-9 nm feature diameters separated by average row spacing of 30 nm.

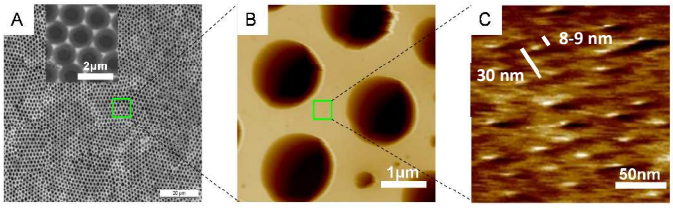

Figure 12. Optical microscopy (A), SEM (A, inset) and AFM (B, C) pictures of honeycomb films obtained from solutions of Dext-*b*-PS_{254} in $CHCl_3$ (15 $g.L^{-1}$) at relative humidity of 50%.

Herein, the higher nanostructure dimensions in comparison with the ones reported in reference 7 are directly correlated to the higher degrees of polymerization of each block, *i.e.* 16 and 254, for both dextran and PS blocks, respectively. This multi-scale ordered porous film represents the first example of hierarchically honeycomb film based on bio-hybrid amphiphilic block copolymer. These diblock copolymers could offer the possibility to create a second nano-porosity by thermal degradation of the dextran block of the sugar-based diblock copolymer.

Conclusions

Novel unprotected dextran-SG1 macro-alkoxyamine have been designed to afford, for the first time, the controlled character of styrene and methyl methacrylate polymerizations by Nitroxide Mediated Polymerization to synthesize amphiphilic diblock copolymers. The ability of dextran-*b*-P(S-*co*-MMA) and dextran-*b*-PS amphiphilic linear block copolymers toward the formation of honeycomb structured films using "Breath Figure" BF technique was investigated. The pore ordering quality of resultant films was characterized by optical microscopy, SEM and AFM. It was concluded that it was not possible to produce ordered pattern of pores in the dextran-*b*-P(S-*co*-PMMA) porous films while dextran-*b*-PS copolymers led to the formation of ordered honeycomb films under suitable

experimental conditions. Such behaviour was discussed in terms of different interfacial tension between the hydrophobic PMMA or PS solution and water droplets. The lower hydrophobicity of PMMA in comparison with PS can reduce the fast polymer precipitation required in the BF process, leading to water droplet coalescence during dextran-*b*-P(S-*co*-MMA) films formation producing non-spherical pores. The use of more hydrophobic dextran-*b*-PS leads to spherical pores, highly organized in a hexagonal pattern. Moreover the high Flory-Huggins interaction parameter χ of the PS/dextran couple induces spontaneously a nanophase separation in between the pores during the fast solvent evaporation, designing a hierarchically structured honeycomb film. The hierarchical structure is due to the dextran-*b*-PS self-assembly into segregated nanodomains which represents the first example of hierarchically honeycomb structured film based on bio-hybrid amphiphilic block copolymer.

Acknowledgements

ANR-10-EQPX-16 XYLOFOREST funding is acknowledged. P. Marcasuzaa, V. Pellerin and A. Khoukh are thanked for their help for AFM, SEM and NMR analyses. The authors thank P. Escalé and P. Marcasuzaa for fruitful discussions.

Notes and references

Université Pau & Pays Adour, CNRS, UMR 5254 – IPREM – Equipe de Physique et Chimie des Polymères, 2 avenue du Président Angot, Pau, F-64053, France. Email: laurent.billon@univ-pau.fr

Electronic Supplementary Information (ESI) available: [^{31}P NMR of mixture of dextran-SG1 and diethyl phosphite, ^{1}H NMR of partial silylated dextran-*b*-PS, calculation of respective degree of polymerization of styrene and MMA units in dextran-*b*-P(MMA$_m$-*co*-S$_n$) copolymers from proton NMR integrations, and theoretical average composition of styrene (F_S) in a P(S-*co*-MMA) copolymer]. See DOI: 10.1039/b000000x/

1. M. Tizzotti, A. Charlot, E. Fleury, M. Stenzel and J. Bernard, *Macromolecular Rapid Communications*, 2010, **31**, 1751.
2. C. Schatz and S. Lecommandoux, *Macromolecular Rapid Communications*, 2010, **31**, 1664.
3. Y. Yang, K. Kataoka and F. M. Winnik, *Macromolecules*, 2005, **38**, 2043.
4. O. S. Hernandez, G. M. Soliman and F. M. Winnik, *Polymer*, 2007, **48**, 921.
5. I. Otsuka, T. Isono, C. Rochas, S. Halila, S. Fort, T. Satoh, T. Kakuchi and R. Borsali, *ACS Macro Letters*, 2012, 1379.
6. I. Otsuka, K. Fuchise, S. Halila, S. b. Fort, K. Aissou, I. Pignot-Paintrand, Y. Chen, A. Narumi, T. Kakuchi and R. Borsali, *Langmuir*, 2010, **26**, 2325.
7. J. D. Cushen, I. Otsuka, C. M. Bates, S. Halila, S. Fort, C. Rochas, J. A. Easley, E. L. Rausch, A. Thio, R. Borsali, C. G. Willson and C. J. Ellison, *ACS Nano*, 2012, **6**, 3424.
8. A. G. Dal Bó, V. Soldi, F. C. Giacomelli, C. Travelet, B. Jean, I. Pignot-Paintrand, R. Borsali and S. Fort, *Langmuir*, 2011, **28**, 1418.
9. C. Schatz, S. Louguet, J.-F. Le Meins and S. Lecommandoux, *Angewandte Chemie International Edition*, 2009, **48**, 2572.
10. Y. S. Kim and J. F. Kadla, *Biomacromolecules*, 2010, **11**, 981.
11. R. Novoa-Carballal and A. H. E. Muller, *Chemical Communications*, 2012, **48**, 3781.
12. K. Loos and R. Stadler, *Macromolecules*, 1997, **30**, 7641.
13. K. Loos and A. H. E. Müller, *Biomacromolecules*, 2002, **3**, 368.
14. K. Akiyoshi, M. Kohara, K. Ito, S. Kitamura and J. Sunamoto, *Macromolecular Rapid Communications*, 1999, **20**, 112.
15. B.-G. Li and L.-M. Zhang, *Carbohydrate Polymers*, 2008, **74**, 390.
16. C. Chauvierre, D. Labarre, P. Couvreur and C. Vauthier, *Macromolecules*, 2003, **36**, 6018.
17. I. Bertholon, S. Lesieur, D. Labarre, M. Besnard and C. Vauthier, *Macromolecules*, 2006, **39**, 3559.
18. D. M. Haddleton and K. Ohno, *Biomacromolecules*, 2000, **1**, 152.
19. C. Houga, J. Giermanska, S. Lecommandoux, R. Borsali, D. Taton, Y. Gnanou and J. F. Le Meins, *Biomacromolecules*, 2009, **10**, 32.
20. S. Yagi, N. Kasuya and K. Fukuda, *Polym J*, 2010, **42**, 342.
21. C. Houga, J.-F. L. Meins, R. Borsali, D. Taton and Y. Gnanou, *Chemical Communications*, 2007, 3063.
22. R. Novoa-Carballal, A. Pfaff and A. H. E. Muller, *Polymer Chemistry*, 2013, **4**, 2278.
23. J. Bernard, M. Save, B. Arathoon and B. Charleux, *Journal of Polymer Science Part A: Polymer Chemistry*, 2008, **46**, 2845.
24. J. Nicolas, Y. Guillaneuf, C. Lefay, D. Bertin, D. Gigmes and B. Charleux, *Progress in Polymer Science*, 2013, **38**, 63.
25. O. García-Valdez, D. G. Ramírez-Wong, E. Saldívar-Guerra and G. Luna-Bárcenas, *Macromolecular Chemistry and Physics*, 2013, **214**, 1396.
26. C. Lefay, Y. Guillaneuf, G. Moreira, J. J. Thevarajah, P. Castignolles, F. Ziarelli, E. Bloch, M. Major, L. Charles, M. Gaborieau, D. Bertin and D. Gigmes, *Polymer Chemistry*, 2013, **4**, 322.
27. T. Kakuchi, A. Narumi, Y. Miura, S. Matsuya, N. Sugimoto, T. Satoh and H. Kaga, *Macromolecules*, 2003, **36**, 3909.
28. M. Hernandez-Guerrero and M. H. Stenzel, *Polymer Chemistry*, 2012, **3**, 563.
29. P. Escalé, L. Rubatat, L. Billon and M. Save, *European Polymer Journal*, 2012, **48**, 1001.
30. H. Ma and J. Hao, *Chemical Society Reviews*, 2011, **40**, 5457.
31. M. Hernández-Guerrero, T. P. Davis, C. Barner-Kowollik and M. H. Stenzel, *European Polymer Journal*, 2005, **41**, 2264.
32. W. Liu, R. Liu, Y. Li, W. Wang, L. Ma, M. Wu and Y. Huang, *Polymer*, 2009, **50**, 2716.
33. J. F. Kadla, F. H. Asfour and B. Bar-Nir, *Biomacromolecules*, 2007, **8**, 161.
34. W. Z. Xu, X. Zhang and J. F. Kadla, *Biomacromolecules*, 2012, **13**, 350.
35. S. R. S. Ting, E. H. Min, P. Escalé, M. Save, L. Billon and M. H. Stenzel, *Macromolecules*, 2009, **42**, 9422.
36. P. Escalé, S. R. S. Ting, A. Khoukh, L. Rubatat, M. Save, M. H. Stenzel and L. Billon, *Macromolecules*, 2011, **44**, 5911.
37. A. S. de León, A. Muñoz-Bonilla, M. Fernández-García and J. Rodríguez-Hernández, *Journal of Polymer Science Part A: Polymer Chemistry*, 2012, **50**, 851.
38. P. Escale, M. Save, A. Lapp, L. Rubatat and L. Billon, *Soft Matter*, 2010, **6**, 3202.

39. P. Escale, L. Rubatat, C. Derail, M. Save and L. Billon, *Macromolecular Rapid Communications*, 2011, **32**, 1072.
40. P. Escale, W. Van Camp, F. Du Prez, L. Rubatat, L. Billon and M. Save, *Polymer Chemistry*, 2013, **4**, 4710.
41. Y. Perez, A. Valdivia, L. Gomez, B. K. Simpson and R. Villalonga, *Macromolecular Bioscience*, 2005, **5**, 1220.
42. J. Vinas, N. Chagneux, D. Gigmes, T. Trimaille, A. Favier and D. Bertin, *Polymer*, 2008, **49**, 3639.
43. I. Ydens, D. Rutot, P. Degée, J.-L. Six, E. Dellacherie and P. Dubois, *Macromolecules*, 2000, **33**, 6713.
44. B. Charleux, J. Nicolas and O. Guerret, *Macromolecules*, 2005, **38**, 5485.
45. J. Nicolas, L. Mueller, C. Dire, K. Matyjaszewski and B. Charleux, *Macromolecules*, 2009, **42**, 4470.
46. C. Dire, J. Belleney, J. Nicolas, D. Bertin, S. Magnet and B. Charleux, *Journal of Polymer Science Part a-Polymer Chemistry*, 2008, **46**, 6333.
47. M. L. Coote, L. P. M. Johnston and M. P. Davis, *Macromolecules*, 1997, **30**, 8191.
48. C. X. Cheng, Y. Tian, Y. Q. Shi, R. P. Tang and F. Xi, *Langmuir*, 2005, **21**, 6576.
49. K. H. Wong, T. P. Davis, C. Barner-Kowollik and M. H. Stenzel, *Polymer*, 2007, **48**, 4950.
50. M. H. Stenzel, C. Barner-Kowollik and T. P. Davis, *Journal of Polymer Science Part a-Polymer Chemistry*, 2006, **44**, 2363.
51. M. H. Stenzel, *Australian Journal of Chemistry*, 2002, **55**, 239.
52. J. Li, J. Peng, W. H. Huang, Y. Wu, J. Fu, Y. Cong, L. J. Xue and Y. C. Han, *Langmuir*, 2005, **21**, 2017.
53. Y. Fukuhira, H. Yabu, K. Ijiro and M. Shimomura, *Soft Matter*, 2009, **5**, 2037.
54. W. D. Harkins and A. Feldman, *Journal of the American Chemical Society*, 1922, **44**, 2665.
55. Y. Wang, B. H. Guo, X. Wan, J. Xu, X. Wang and Y. P. Zhang, *Polymer*, 2009, **50**, 3361.
56. G. Widawski, M. Rawiso and B. Francois, *Nature*, 1994, **369**, 387.
57. M. Srinivasarao, D. Collings, A. Philips and S. Patel, *Science*, 2001, **292**, 79.
58. U. H. F. Bunz, *Advanced Materials*, 2006, **18**, 973.
59. M. H. Stenzel and T. P. Davis, *Australian Journal of Chemistry*, 2003, **56**, 1035.
60. A. Nygard, T. P. Davis, C. Barner-Kowollik and M. H. Stenzel, *Australian Journal of Chemistry*, 2005, **58**, 595.
61. B. de Boer, U. Stalmach, H. Nijland and G. Hadziioannou, *Advanced Materials*, 2000, **12**, 1581.
62. X. Hao, M. H. Stenzel, C. Barner-Kowollik, T. P. Davis and E. Evans, *Polymer*, 2004, **45**, 7401.
63. T. Hayakawa and S. Horiuchi, *Angewandte Chemie International Edition*, 2003, **42**, 2285.
64. J. Li, Q.-L. Zhao, J.-Z. Chen, L. Li, J. Huang, Z. Ma and Y.-W. Zhong, *Polymer Chemistry*, 2010, **1**, 164.
65. B.-B. Ke, L.-S. Wan, W.-X. Zhang and Z.-K. Xu, *Polymer*, 2010, **51**, 2168.
66. M.V. Walter, P. Lundberg, D. Hult, A. Hult, M. Malkoch, *Polymer Chemistry*, 2013, **4**, 2680.